arXiv:1009.0356v1 [cond-mat.stat-mech] 2 Sep 2010

Non-Kosterlitz-Thouless transitions for the q-state clock models

Seung Ki Baek* and Petter Minnhagen

Department of Physics, Umeå University, 901 87 Umeå, Sweden

Abstract

The q-state clock model with the cosine potential has a single phase transition for $q \leq 4$ and two transitions for $q \geq 5$. It is shown by Monte Carlo simulations that the helicity modulus for the five-state clock model ($q = 5$) does not vanish at the high-temperature transition. This is in contrast to the clock models with $q \geq 6$ for which the helicity modulus vanishes. This means that the transition for the five-state clock model differs from the Kosterlitz-Thouless (KT) transition. It is also shown that this change in the transition is caused by an interplay between the number of angular directions and the interaction potential: by slightly modifying the interaction potential, the KT transition for $q = 6$ turns into the same non-KT transition. Likewise, the KT transition is recovered for $q = 5$ when the Villain potential is used. Comparisons with other clock-model results are made and discussed.

PACS numbers: 05.70.Fh,64.60.Cn,75.40.Cx

*Corresponding author, E-mail: garuda@tp.umu.se

I. INTRODUCTION

The research on two-dimensional (2D) continuous phase transition has a long history. One of the corner stones was Onsager's solution of the 2D Ising model [1] which led to the understanding of the connection between a broken symmetry and the universality of a continuous phase transition [1]. Another corner stone was the discovery of a 2D topological phase transition by Kosterlitz and Thouless (KT) [2, 3]. This topological transition does not involve any broken symmetry and has hence a completely different character. The q-state clock models have the interesting feature that both of these types of phase transitions are possible and to some extent interfere with each other. Partly because of this, the phase diagram for the q-state clock model is a longstanding question with as yet no clear consensus, both as regarding the number of phase transitions and the character of the phase transitions [4–11]. The overall feature, for which there is full consensus, is that for $q \leq 4$, there is only one transition, whereas for $q \geq q_c$ there are two transitions. However, the value of q_c has been suggested to be both $q_c = 5$ as in Refs. [4–7] and $q_c = 6$ as in Refs. [8, 9]. The most common view is that $q_c = 5$ and that the two phase transitions for $q \geq 5$ are of the KT type [4–7]. If there is only one transition for $q = 5$ as suggested in Refs. [8, 9], it should be discontinuous [6]. More recently, it has been suggested that the upper transition for the six-state clock model is not the KT transition [10, 11]. Quite to the contrary, however, this transition was later found to be of the KT type in Ref. [12].

In the present paper, we reinvestigate the transitions for $q = 4, 5$, and 6, using Monte Carlo (MC) simulations. It is found that the five-state clock model has two separate transitions. However, the upper transition is not a pure KT transition, since the helicity modulus does not vanish at the transition. It is also found that if the interaction potential is changed to the Villain potential, then the upper transition does become a pure KT transition. In a similar way, it is found that the six-state clock model has the KT transition and that it turns into a non-KT transition when the potential is slightly changed. If the potential is further changed the upper and lower phase transitions coalesce into one and become discontinuous. Thus both the number of phase transitions and the character of the transitions for a clock model with $q \geq 5$ depend on the precise shape of the potential. This work is organized as follows: Sec. II introduces the spin models and statistical quantities we are investigating. These models have somewhat different interaction potentials between spins

but have the same symmetry and quadratic leading term. We present our main numerical results in Sec. III and summarize them in Sec. IV.

II. CLOCK MODELS AND HELICITY MODULUS

The q-state clock model is, like the Ising model, a model of interacting spins where the interaction energy between two neighboring spins is determined by the difference in spin angles. Hence we begin with a Hamiltonian derived from a spin-interaction potential U as

$$H = \sum_{\langle ij \rangle} U(\theta_i - \theta_j), \tag{1}$$

where θ_i is the ith spin angle, and the sum runs over all the nearest-neighbor pairs. We will here consider the case when the lattice is a 2D $L \times L$ square lattice. The interaction potential for the clock model is given by

$$U(\phi) = V(\phi) \equiv -J \cos\phi, \tag{2}$$

where J is the coupling constant. Each spin can only have q discrete directions, $\theta = 0, \frac{2\pi}{q}, \ldots, \frac{2\pi(q-1)}{q}$. This means that the q-state clock model has a discrete Z_q symmetry. In case of the Ising model, $q = 2$, the possible spin directions are $\theta = 0$ and π, corresponding to the usual spin-up and spin-down directions, and the symmetry is Z_2. In the limit $q \to \infty$, the spin angles θ_i becomes continuous and the Hamiltonian recovers a full $U(1)$ symmetry. This limiting model is called the 2D XY model and is the prototype of a system exhibiting the KT transition.

The critical properties of a continuous phase transition is to a large extent determined by the symmetry and the dimension of the model. Thus it is reasonable to assume that a small change in the interaction potential $V(\phi)$ will not matter as long as the Z_q symmetry is preserved. Such a change is given by the Villain approximation [13],

$$U(\phi) = V_{\text{Villain}}(\phi) \equiv -\frac{1}{\beta} \ln \left\{ \sum_{n=-\infty}^{\infty} \exp\left[-\beta(\phi - 2\pi n)^2/2\right) \right\}, \tag{3}$$

where β is the inverse of temperature T in units such that the Boltzmann constant is unity. Figure 1 compares the clock-model potential $V(\phi)$ with the Villain approximation. The point with the Villain approximation is that this approximation makes theoretical analysis

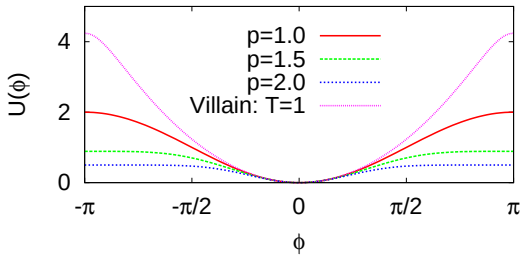


FIG. 1: (Color online) Interaction potentials in Eq. (4) at various p values, compared with the Villain approximation, Eq. (3).

more tractable [4] and it has often been tacitly assumed that the phase diagram and phase-transition properties obtained within the Villain approximation should be universal and also valid for the clock-model potential, Eq. (2) [4, 5].

In order to investigate the sensitivity to the precise functional form $V(\phi)$ in a systematic way, one can use the following parameterization [14, 15]

$$U(\phi) = V_p(\phi) \equiv \frac{2J}{p^2}\left[1 - \cos^{2p^2}\left(\frac{\phi}{2}\right)\right], \tag{4}$$

Note that $V_{p=1} - J = -J\cos\phi = V(\phi)$. For $p > 1$ the potential has a smaller dip, and for $p < 1$ a larger dip, as is shown in Fig. 1. Also note that for small ϕ, the leading term $J\phi^2/2$ is quadratic and is identical for V, $V_{\rm Villain}$, and V_p.

In the present paper, we will focus on the helicity modulus which measures the resistance with respect to a uniform twist across the sample in one direction. For a twist of size Δ_x across the x direction, this means that the Hamiltonian in the presence of the twist field is given by $H(\Delta_x) = \sum_{\langle i,j\rangle} V_p(\theta_i - \theta_j - \Delta_x/L_x)$, where $L_x = L$ is the system size in the x direction. The helicity modulus Υ measures the increase of the free energy F caused by the twist in the limit of small Δ_x. This increment is given by $\frac{\partial^2 F}{\partial \Delta_x^2}|_{\Delta_x=0}\Delta_x^2/2 \equiv \Upsilon\Delta_x^2/2$, where the leading dependence in Δ_x is of the second order since a twist will always increase the free energy or leave it invariant. For an interaction potential $U(\phi)$, the helicity modulus is given by

$$\Upsilon = \langle e\rangle - L^2\beta\left\langle s^2\right\rangle, \tag{5}$$

with $e \equiv L^{-2}\sum_{\langle ij\rangle_x} U''(\theta_i - \theta_j)$ and $s \equiv L^{-2}\sum_{\langle ij\rangle_x} U'(\theta_i - \theta_j)$ where the sum is over all links in the x direction. The derivatives are with respect to the argument ϕ so that $U'(\phi) \equiv \partial U/\partial\phi$ and $U'' \equiv \partial^2 U/\partial\phi^2$. We will here also study a higher-order correlation function

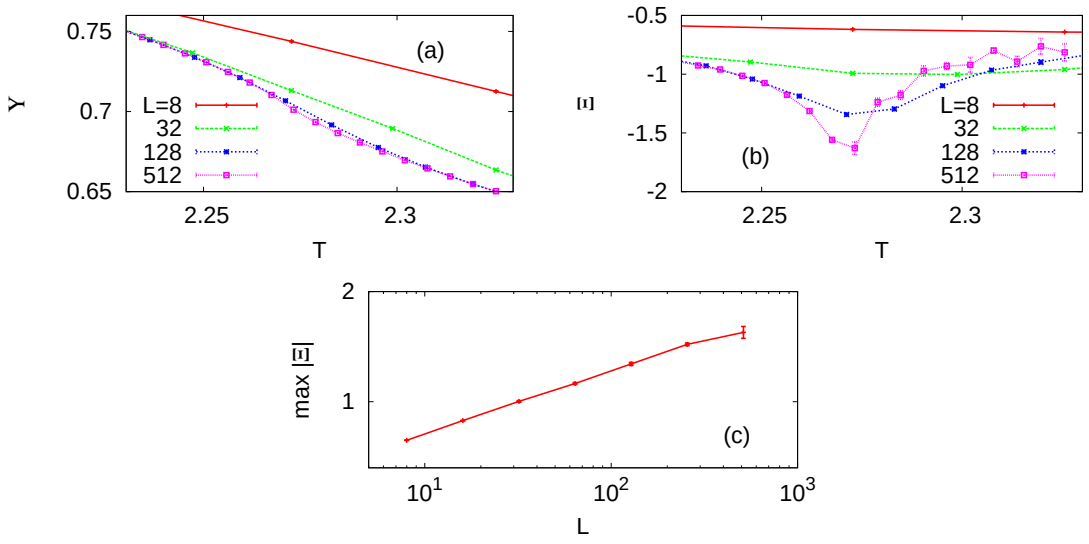


FIG. 2: (Color online) 2D Ising model ($q = 2$). (a) Helicity modulus and (b) its temperature derivative. (c) The peak heights of Ξ shows a logarithmic growth with the system size (see text). Error bars are shown in all of these plots.

$\Xi \equiv \partial\Upsilon/\partial T = -\beta^2 \partial\Upsilon/\partial\beta$ written as

$$\Xi = \beta^2 \left\{ \langle eH \rangle - \langle e \rangle \langle H \rangle + L^2 \left\langle s^2 \right\rangle - L^2 \beta \left[\left\langle s^2 H \right\rangle - \left\langle s^2 \right\rangle \langle H \rangle \right] \right\}, \tag{6}$$

and check its size dependence $\Xi \sim L^{\alpha_h}$ through MC simulations.

III. MONTE CARLO SIMULATIONS

We use the Wolff single-cluster algorithm [16] throughout this work. All the measurements presented here have been obtained by updating clusters $O(10^6)$ up to $O(10^7)$ times after equilibration. In Fig. 2(a), we illustrate our calculations for the two-state clock model, which corresponds to the 2D Ising model. At the Ising transition, the helicity modulus makes a transition from a higher to a lower value. However, the helicity modulus remains positive and nonzero for all temperatures. This is in contrast to the KT transition for which the helicity modulus is zero in the high-temperature phase. The Ising criticality is instead reflected in the helicity modulus by the fact that its temperature derivative diverges at the critical temperature. This divergence is directly picked up by the correlation function Ξ, as illustrated in Fig. 2(b). From the peak heights in Fig. 2(b), one can determine the size scaling $\Xi \sim L^{\alpha_h}$ and the critical index α_h. Figure 2(c) illustrates that $\alpha_h = 0$ for the Ising

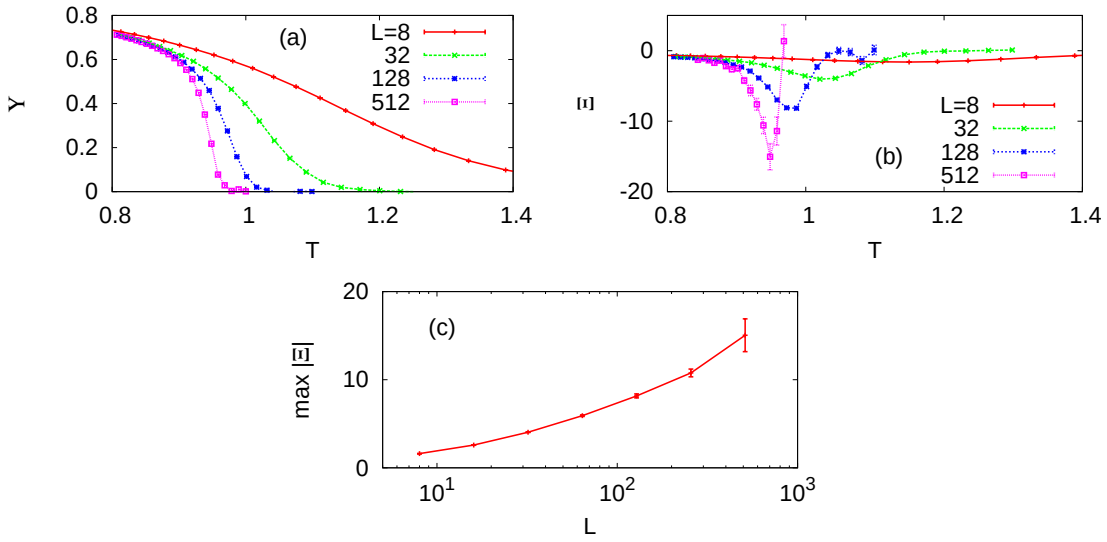


FIG. 3: (Color online) 2D XY model ($q = \infty$). (a) Helicity modulus and (b) its temperature derivative. (c) The peak heights of Ξ shows a divergence as L grows. Error bars are also shown.

model since peak heights are consistent with a logarithmic growth. For the Ising model, this is a trivial result since all correlations involving s vanishes by $s = 0$. This mean that Ξ is proportional to the specific heat for the Ising model and hence $\alpha_h = \alpha/\nu = 0$.

The other extreme for the clock models is the limiting case $q = \infty$, which corresponds to the 2D XY model, the prototype model for the KT transition. Figure 3(a) shows the helicity modulus in the 2D XY model for various sizes L. The characteristics for the helicity modulus in case of the KT transition is that it jumps from a finite value $2T_c/\pi$ to zero at T_c in the limit $L = \infty$ [17, 18]. Figure 3(a) is consistent with such a behavior. Figure 3(b) illustrates that the peak heights of Ξ diverges and the divergence is again shown to be consistent with a logarithmic growth [Fig. 3(c)]. The reason is, however, different since the correlation length ξ for the KT transition diverges as $\ln \xi \propto (T - T_c)^{-1/2}$ [3]. At the same time, Ξ is proportional to $|T - T_c|^{-1/2}$ [19], leading to the size scaling $\Xi \sim \ln L$. Our MC simulations suggest that Ξ for all q are consistent with at least a logarithmic size divergence [see Fig. 4(e)]. However, our MC simulations do not have enough precision at the largest sizes to rule out a stronger divergence in a power-law form. The crucial point in the present context is that the correlation function Ξ displays a phase-transition singularity, manifested in a size divergence, for *all* the clock models including the Ising and the XY model.

In Fig. 4, we present the results for $q = 3, 4, 5$, and 6. For each q, the helicity modulus Υ

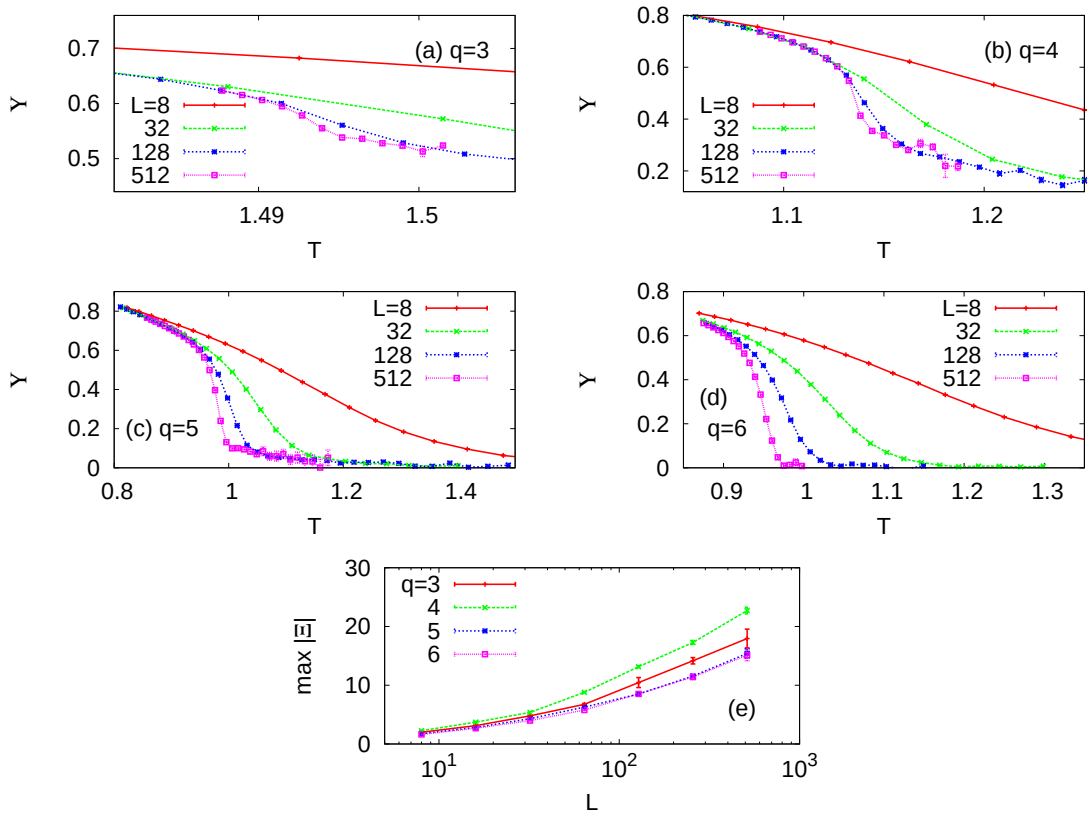


FIG. 4: (Color online) Helicity modulus measured for clock models with (a) $q = 3$, (b) $q = 4$, (c) $q = 5$, and (d) $q = 6$, together with error bars. (e) The peak heights of Ξ at the q values.

and the higher-order correlation function Ξ are given. Figure 4(e) shows that for all q, Ξ has a critical divergence. This means that in all cases there exists a phase transition which can be associated with the helicity. An interesting point to note is that for $q = 2, 3, 4$, *and* 5, the helicity modulus itself remains finite for all temperatures. This means that in these four cases the transition is *not* of the KT type. The clock models with $q = 2, 3$, and 4 undergo well-known phase transitions: for $q = 2$ this is the Ising transition, for $q = 3$ the three-state Potts transition [20] and for $q = 4$ again an Ising-like transition [21]. These transitions go directly from the low-temperature to the high-temperature phase, which rules out the possibility for two consecutive transitions separated by a quasicritical phase characterized by a power-law decay of spin correlations. However, theoretical predictions strongly suggest that the five-state clock model does have two transitions [4–7]. This is also what we find from our simulations: Fig. 5(a) determines the lower transition using the order parameter

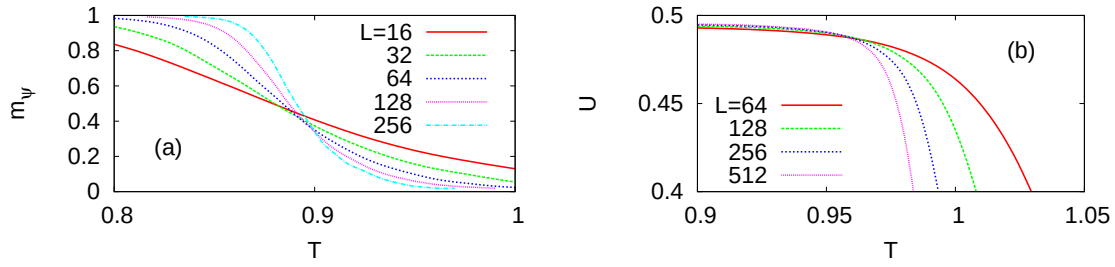


FIG. 5: (Color online) (a) The order parameter in Eq. (7) around the lower transition temperature for the five-state clock model. Note that the crossing points between curves move slightly to the right as the size becomes larger. (b) Merging of Binder's cumulant around the higher transition point for the same model.

introduced in Ref. [15],

$$m_\psi \equiv \langle \cos(q\psi) \rangle \,, \tag{7}$$

where ψ means the phase of the magnetization vector so that $\mathbf{m} \equiv L^{-2} \sum_j e^{i\theta_j} = |m| e^{i\psi}$. This parameter distinguishes the true long-range order from the quasi-long-range order. On the other hand, Fig. 5(b) detects the upper transition, at which the spin-correlations start to decay exponentially, using Binder's cumulant,

$$U \equiv 1 - \frac{\langle |m|^4 \rangle}{2 \langle |m|^2 \rangle^2}. \tag{8}$$

These measurements show that there are indeed two separated transitions. Thus the conclusion for the five-state clock model is that it does have two consecutive transitions. However, contrary to the theoretical expectations in Refs. [4–7], it is not the KT transition since as is illustrated in Fig. 4(c), the helicity modulus remains finite for all temperatures precisely as for $q = 2, 3$, and 4. Nor is it a discontinuous transition since we do not observe any double peaks in the energy distribution [15].

In order to better understand the reason for this, we first note that the conclusions in Refs. [4, 5, 7] were obtained using the Villain approximation. In Fig. 6(a), we show the result for the helicity modulus for the five-state clock model using the Villain potential (compare Fig. 1). In this case, the helicity modulus does indeed vanish. This means that, in accordance with Refs. [4–7], the five-state clock model within the Villain approximation does have two consecutive transitions where the higher one is the KT transition. The crucial point made here is that this is not true for the real five-state clock model. The reason for

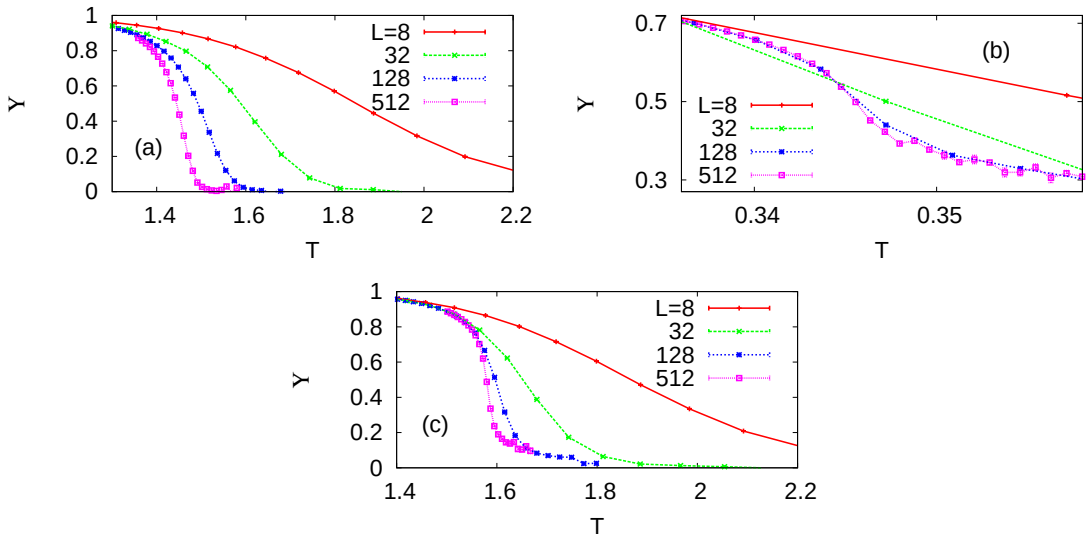


FIG. 6: (Color online) The helicity modulus for (a) the five-state Villain model, (b) the generalized six-state clock model with $p = 2.0$, and (c) the four-state Villain model. Error bars are shown but usually smaller than the symbol sizes.

this change in the transition is clearly the interplay between the number of clock states, q, and the detailed shape of the potential. This is further illustrated in Fig. 6(b), which shows the helicity modulus for the six-state clock model using the generalized potential in Eq. (4) with $p = 2.0$, which gives a slightly flatter potential (Fig. 1). For this potential, the six-state clock model has two consecutive transitions where the helicity modulus does not vanish at the upper transition, just as for the five-state clock model with the usual cosine potential. However, the six-state clock model has two consecutive transitions where the upper one is the KT transition both for the usual cosine potential [Fig. 4(d)] and for the Villain potential. Figure 6(c) shows the helicity modulus for the four-state clock model within the Villain approximation. However, in this case, the helicity modulus remains nonzero for all temperatures as for the usual cosine potential.

IV. CONCLUSIONS

From numerical simulations, it was verified that the five-state clock model has two transitions. It was also found that the helicity modulus Υ does not vanish at the upper transition. Yet it was found that the helicity modulus does vanish at the upper transition provided

the cosine potential is replaced by the Villain potential. In this latter case, the transition is perfectly consistent with the standard KT transition. Heuristically, this transition can be interpreted in terms of the unbinding of vortex-antivortex pairs: below the transition temperature, these pairs are bound together whereas above it the effective vortex-anivortex attractive interaction is softened such that free unbound vortices appear. It is the presence of such free vortices which is signaled by the vanishing of Υ [17–19]. It seems plausible that a description of the phase transition in terms of vortex-antivortex pairs will remain adequate even after the tiny change from the Villain potential to the usual clock-model potential. If so, this means that the rapid drop of Υ at the transition for the five-state clock model is again associated with a softening of the effective vortex-antivortex interaction, with the important difference that this softening is not enough to create free vortices. In this interpretation, it is the lack of free vortices which forces Υ to remain finite for all temperatures. Whether or not the softening will be enough to create free vortices then depends on an intricate balance between the number of clock states, q, and the precise form of the potential. This interpretation is consistent with the finding that, whereas the six-state clock model undergoes the KT transition for which the helicity modulus vanishes, it only takes a small modification of the potential using the systematic parameterization in Eq. (4) to change the transition such that the helicity modulus does not vanish. From this perspective, the topological transition of the five-state clock model, for which the helicity modulus does not vanish, appears to be a new and weaker cousin of the proper KT transition.

Acknowledgments

We acknowledge the support from the Swedish Research Council with the Grant No. 621-2002-4135. This research was conducted using the resources of High Performance Computing Center North (HPC2N).

---

[1] C. Domb, *The Critical Point* (Taylor & Francis, London, 1996).

[2] J. M. Kosterlitz and D. J. Thouless, J. Phys. C **6**, 1181 (1973).

[3] J. M. Kosterlitz, J. Phys. C **7**, 1046 (1974).

[4] J. V. José, L. P. Kadanoff, S. Kirkpatrick, and D. R. Nelson, Phys. Rev. B **16**, 1217 (1977).

[5] S. Elitzur, R. B. Pearson, and J. Shigemitsu, Phys. Rev. D **19**, 3698 (1979).

[6] E. Domany, D. Mukamel, and A. Schwimmner, J. Phys. A **13**, L311 (1980).

[7] J. L. Cardy, J. Phys. A **13**, 1507 (1980).

[8] P. Ruján, G. O. Williams, H. L. Frisch, and G. Forgács, Phys. Rev. B **23**, 1362 (1981).

[9] H. H. Roomany and H. W. Wyld, Phys. Rev. B **23**, 1357 (1981).

[10] C. M. Lapilli, P. Pfeifer, and C. Wexler, Phys. Rev. Lett. **96**, 140603 (2006).

[11] C.-O. Hwang, Phys. Rev. E **80**, 042103 (2009).

[12] S. K. Baek, P. Minnhagen, and B. J. Kim, Phys. Rev. E **81**, 063101 (2010).

[13] J. Villain, J. Phys. (France) **36**, 581 (1975).

[14] E. Domany, M. Schick, and R. H. Swendsen, Phys. Rev. Lett. **52**, 1535 (1984).

[15] S. K. Baek, P. Minnhagen, and B. J. Kim, Phys. Rev. E **80**, 060101(R) (2009).

[16] U. Wolff, Phys. Rev. Lett. **62**, 361 (1989).

[17] D. R. Nelson and J. M. Kosterlitz, Phys. Rev. Lett. **39**, 1201 (1977).

[18] P. Minnhagen and G. G. Warren, Phys. Rev. B **24**, 2526 (1981).

[19] P. Minnhagen, Rev. Mod. Phys. **59**, 1001 (1987).

[20] F. Y. Wu, Rev. Mod. Phys. **54**, 235 (1982).

[21] M. Suzuki, Prog. Theor. Phys. **37**, 770 (1967).